Epitaxial Growth of ϵ-Fe_2O_3 on Mullite Found through Studies on a Traditional Japanese Stoneware

Yoshihiro Kusano,*[,†] Tatsuo Fujii,[‡] Jun Takada,[‡] Minoru Fukuhara,[§] Akira Doi,[†] Yasunori Ikeda,[+] and Mikio Takano[+]

Department of Applied Arts and Design, Kurashiki University of Science and the Arts, 2640 Nishinoura, Tsurajima-cho, Kurashiki-shi, Okayama 712-8505, Japan, Department of Applied Chemistry, Okayama University, 3-1-1 Tsushima-naka, Okayama 700-8530, Japan, Department of Applied Chemistry, Okayama University of Science, 1-1 Ridai-cho, Okayama 700-0005, Japan, and Institute for Chemical Research, Kyoto University, Uji, Kyoto-fu 611-0011, Japan

Received August 16, 2007

In the course of our study on a Japanese traditional stoneware called "Bizen", we have found that ϵ-Fe_2O_3, which has been classically known but recently limelighted for its magnetic potentiality, crystallizes epitaxially on needlelike crystals of mullite, $3(Al,Fe)_2O_3 \cdot 2SiO_2$. This interesting reaction occurred when a pellet of Bizen clay powder was covered with rice straw and then heated to 1250 °C in a stream of nitrogen containing 1−2 vol % of oxygen. It is known that mullite forms from the clay on heating and that the rice straw provides potassium to induce partial melting in the pellet surface to a depth of ~50 μm. The ϵ-Fe_2O_3-on-mullite particles formed in this molten region, changing their morphology with the oxygen partial pressure. Square-columnar single-crystalline particles with prismatic ends grew to $\sim 0.1 \times 0.1 \times 0.5\ \mu m^3$ at $N_2/O_2 = 99/1$, while dendritic finlike crystals of $\sim 0.3 \times 0.1 \times 0.8\ \mu m^3$, which was then the biggest size ever reported, grew at $N_2/O_2 = 98/2$. The relative ϵ-Fe_2O_3-to-mullite orientation also changed with the oxygen partial pressure. This discovery suggests morphological controllability of this metastable but magnetically interesting iron oxide as a function of the oxygen partial pressure.

Introduction

The Bizen stoneware, an artistic Japanese unglazed ceramics, has been loved for over one thousand years for their practical and artistic merits. The Bizen art is considered to be an "art of clay and flame" because the different colors of red, orange, purple, yellow, black, silver, and gold appear in various forms without the aid of artificial glazing or dyeing figures. In a previous paper,[1] we studied the formation mechanism of "Hidasuki", a characteristic reddish pattern appearing specifically where the clay contacts rice straw, which is used as a separator to prevent thermal adhesion of stoneware in a kiln. When heated, the rice straw provides the stoneware surface with potassium to induce partial melting to a depth of about 50 μm. This melting generates special circumstances where mullite, $3(Al,Fe)_2O_3 \cdot 2SiO_2$, which is otherwise the dominant phase, is replaced by corundum (α-Al_2O_3), hematite (α-Fe_2O_3), and others. Stating in due order, the corundum first precipitates in the liquid as hexagonal platelike crystals, on the edges of which the hematite precipitates epitaxially. The hematite continues to grow so that the primary corundum crystals are wholly covered to form a specific single-crystalline α-Fe_2O_3/α-Al_2O_3/α-Fe_2O_3 structure, and the contribution of this unique microstructure to coloring was discussed. With this knowledge of the formation mechanism, we could reproduce the Hidasuki pattern in the form of written characters.

The Bizen clay contains Fe in a high amount of 3 wt % as Fe_2O_3. In a further study, we have noticed that the behavior of Fe in the molten region strongly depends on the oxygen partial pressure during heating (p_{O_2}) and that ϵ-Fe_2O_3 forms in place of α-Fe_2O_3 at relatively low p_{O_2} values. The ϵ-oxide was discovered by Forestier and Guiot-Guillain in 1934[2] but had been known much less than α- and γ-Fe_2O_3 until it began to attract much attention for its potential as a magnetic material: This oxide is a ferrimagnet featured by a T_N of ~490 K, a relatively small magnetization of ~0.25 μ_B/Fe, and a very high coercivity of 20 kOe at room temperature.[3–13] However, this oxide has been obtainable only as very fine

* To whom correspondence should be addressed. Tel and Fax: +81 86 440 1051. E-mail: yoshi-k@arts.kusa.ac.jp.
† Kurashiki University of Science and the Arts.
‡ Okayama University.
§ Okayama University of Science.
+ Kyoto University.

(1) Kusano, Y.; Fukuhara, M.; Fujii, T.; Takada, J.; Murakami, R.; Doi, A.; Anthony, L.; Ikeda, Y.; Takano, M. *Chem. Mater.* **2004**, *16*, 3641.
(2) Forestier, H.; Guiot-Guillain, G. C. R. *Acad. Sci. (Paris)* **1934**, *199*, 720.
(3) Schrader, R.; Büttner, G. *Z. Anorg. Allg. Chem.* **1963**, *320*, 220.
(4) Dézsi, I.; Coey, J. M. D. *Phys. Status Solidi* **1973**, *15*, 681.
(5) Jin, J.; Ohkoshi, S.; Hashimoto, K. *Adv. Mater.* **2004**, *16*, 48.
(6) Tronc, T.; Chanéac, C.; Jolivet, J. P. *J. Solid State Chem.* **1998**, *139*, 93.
(7) Dormann, J. L.; Viart, N.; Rehspringer, J. L.; Ezzir, A.; Niznansky, D. *Hyperfine Interact.* **1998**, *112*, 89.
(8) Popovici, M.; Gich, M.; Nižnanský, D.; Roig, A.; Savii, C.; Casas, L.; Molins, E.; Zaveta, K.; Enache, C.; Sort, J.; de Brion, S.; Chouteau, G.; Nogués, J. *Chem. Mater.* **2004**, *16*, 5542.

10.1021/cm7023247 CCC: $40.75
Published on Web 12/11/2007

particles of 100–140 nm in length and 20–40 nm in width, typically, embedded in a massive matrix of amorphous silica. From the thermal behavior and also from such a structural feature that the ferric ions are coordinated both octahedrally and tetrahedrally, this phase has been understood to be an intermediary metastable phase appearing on the way of transformation from γ-Fe_2O_3 of the spinel type to α-Fe_2O_3 of the corundum type.[6] In this paper, we report an unprecedented, quite specific formation process of this potential material.

Experimental Procedures

The main crystalline phases contained in the starting Bizen clay are quartz (SiO_2), halloysite ($Al_2O_3 \cdot 2SiO_2 \cdot 4H_2O$), montmorillonite ($(Na,Ca)_{0.33}(Al,Mg)_2(Si_4O_{10})(OH)_2 \cdot nH_2O$), and feldspar ($(Na,K)AlSi_3O_8$). Clay powder of less than $\sim 10^2$ μm in diameter was pelletized to 20 mm in diameter and 2 mm in thickness, covered with rice straw, and heated up to 1250 °C at a rate of 1 °C/min in a stream of N_2/O_2 mixed gas. Then, the pellet was cooled to 800 °C at the same rate and down to room temperature more rapidly. Microstructural observations were carried out with scanning electron microscopy [SEM; Hitachi S-4300 equipped with an energy-dispersive X-ray spectrometer (EDS)] and also with transmission electron microscopy (TEM; JEOL JEM-4000EX and Topcon EM-002B equipped with an EDS). For these observations, the crystalline phases formed in the surface region were isolated from the glassy matrix by treating the sample surface with 1 M hydrofluoric acid for 5 min, dispersed in carbon tetrachloride, and collected on a microgrid. Phase identification was carried out also by using powder X-ray diffraction (Rigaku RINT 2500V) and electron diffraction (ED; JEM-4000EX). Simulations of ED patterns were carried out using the multislice simulation software *MacTempas*.

Results and Discussion

The pellet surface became yellowish-orange and brownish-red after the heat treatment at $N_2/O_2 = 99/1$ (N99O1) and 98/2 (N98O2), respectively. As compared in parts a and b of Figure 1, the crystalline phases collected from the N99O1 surface were mostly needlelike particles but those from the N98O2 surface were dominated by the aforementioned platelike α-Fe_2O_3/α-Al_2O_3/α-Fe_2O_3 particles.

TEM observations and EDS measurements have indicated consistently that the needles commonly seen in parts a and b of Figure 1 are single crystals of mullite grown along a specific axis. However, these are all conglutinated by small particles, as shown in Figure 2a for N99O1 first. These parasitic crystals are not mullite. The EDS spectrum of Figure 2b taken from a parasite-free part of a mullite crystal showed the presence of Al, Si, and a small amount of Fe as expected from the mullite composition of $3(Al,Fe)_2O_3 \cdot 2SiO_2$, but the spectrum of Figure 2c from a parasitic particle indicates an iron oxide. Moreover, ED results on the parasite, such as is shown in Figure 3a, indicated an orthorhombic structure, not the trigonal α-Fe_2O_3 structure. The lattice constants and the reflection conditions deduced were consistent with the literature data for ϵ-Fe_2O_3 of $Pna2_1$ and a_ϵ, b_ϵ, and c_ϵ = 0.5095, 0.8789, and 0.9437 nm, respectively.[6] Simulations based on these literature data are surely in excellent consistency with the experimental pattern, as compared in parts a and b of Figure 3, typically. We thus conclude here that the fine particles parasitic to mullite are single crystals of ϵ-Fe_2O_3. These crystals commonly have a square-columnar shape with prismatic ends, such as is seen in Figure 4, where the same pair of ϵ-Fe_2O_3 particles are observed from different angles using SEM and TEM.

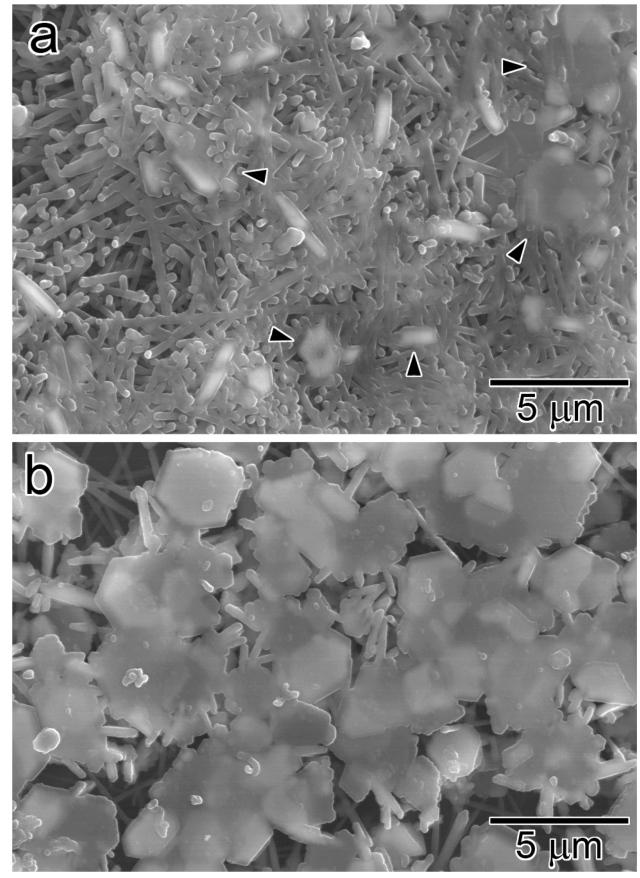

Figure 1. SEM images of the crystals collected from the surfaces of N99O1 (a) and N98O2 (b). In part a, the α-Fe_2O_3/α-Al_2O_3/α-Fe_2O_3 particles are rather rare, as pointed to with arrow heads here and there, while they are dominant in part b. The needlelike crystals are mullite.

The ϵ-oxide remarkably changes its crystal shape and size with p_{O_2}. When N99O1 and N98O2 are compared, those in the latter are larger in size, dendritic, and thin finlike in shape, as seen in Figure 5. The maximum size of $\sim 0.3 \times 0.1 \times 0.8$ μm^3 that we observed is considerably larger than the typical size of $\sim 0.04 \times 0.04 \times 0.14$ μm^3 reported in the previous studies. Another notable thing is twinning, such as is seen in Figure 5b. The combination of dendritic shape and twinning suggests that a slight increase of p_{O_2} resulted in a rapid growth. Further experiments under finely controlled p_{O_2} values must be very interesting.

(9) Gich, M.; Roig, A.; Frontera, C.; Moling, E.; Sort, J.; Popovici, M.; Chouteau, G.; Martín y Marero, D.; Nogués, J. *J. Appl. Phys.* **2005**, *98*, 044307.
(10) Tronc, E.; Chanéac, C.; Jolivet, J. P.; Grenèche, J. M. *J. Appl. Phys.* **2005**, *98*, 053901.
(11) Kurmoo, M.; Rehspringer, J. L.; Hutlova, A.; D'Orléans, C.; Vilminot, S.; Estournès, C.; Niznansky, D. *Chem. Mater.* **2005**, *17*, 1106.
(12) Ohkoshi, S.; Sakurai, S.; Jin, J.; Hashimoto, K. *J. Appl. Phys.* **2005**, *97*, 10K312.
(13) Sakurai, S.; Jin, J.; Hashimoto, K.; Ohkoshi, S. *J. Phys. Soc. Jpn.* **2005**, *74*, 1946.

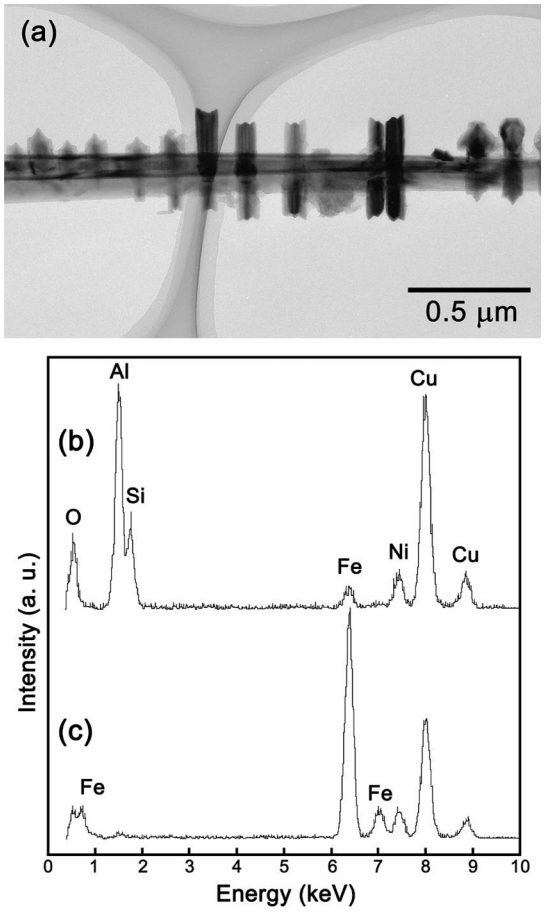

Figure 2. Typical TEM image for N99O1 (a) and the EDS spectra from a needlelike crystal (b) and a parasitic fine particle (c). Spectrum c indicates that the fine particles are an iron oxide, where the small extra peaks indicating Cu and Ni are from the sample holder and the Al peak is from the carrier particle, mullite.

Here we compare the structural features of ϵ-Fe_2O_3 and mullite. Mullite has an orthorhombic unit cell of *Pbam* with $a_m = 0.7546$ nm, $b_m = 0.7690$ nm, and $c_m = 0.2884$ nm (JCPDS No. 15-0776), in which chains made of edge-sharing AlO_6 octahedra run along the *c* axis at each corner and at the center as well, as illustrated in Figure 6a. These chains are linked to $(Al,Si)O_4$ tetrahedra through corner sharing. It is known that Fe can partially replace the Al at the octahedral site mainly and expands the cell volume slightly.[14–22] The Fe-containing mullite in the present samples has lattice constants of $a_m = 0.7553(2)$ nm, $b_m = 0.7703(5)$ nm, and $c_m = 0.2894(0)$ nm. In the orthorhombic unit cell of ϵ-Fe_2O_3 ($Pna2_1$, $a_\epsilon = 0.5095$ nm, $b_\epsilon = 0.8789$ nm, and $c_\epsilon = 0.9437$ nm), triple chains made of edge-sharing FeO_6 octahedra run along the a_ϵ axis. These chains are connected to each other by sharing corners of the FeO_6 octahedra, and the resulting one-dimensional cavities are occupied by chains of corner-sharing FeO_4 tetrahedra (Figure 6b). Thus, the mixing of octahedral and tetrahedral units and their linkage through corner sharing are common to these oxides, but the overall arrangements of these polyhedra are rather different. However, these phases are connected epitaxially as described below.

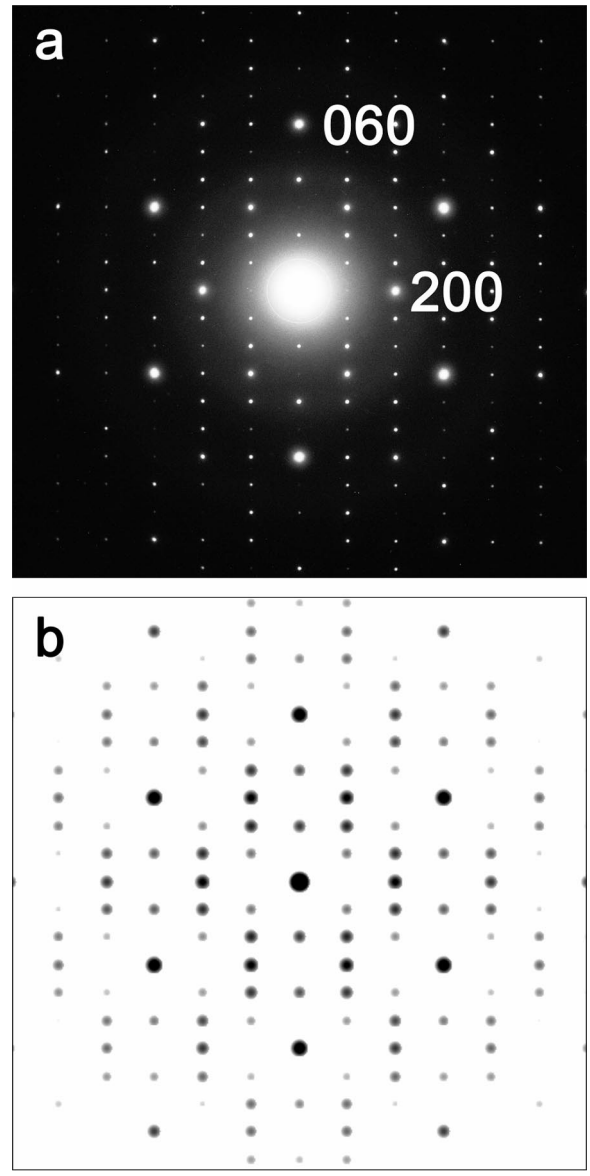

Figure 3. (a) Typical [001] ED pattern taken from a parasitic iron oxide particle seen in Figure 2a. (b) [001] ED pattern calculated using the crystal data described in the literature[6] and a crystal thickness $t = 5$ nm. The excellent agreement between these indicates that the parasite is ϵ-Fe_2O_3.

The relative ϵ-Fe_2O_3-to-mullite orientation was studied by means of ED. The pattern of Figure 7a taken from N99O1 indicates that the zone axis of $[1\bar{1}0]$ for mullite corresponds to the $[\bar{1}01]$ zone axis for ϵ-Fe_2O_3. The crystallographic relations deduced here are $c_m \parallel b_\epsilon$ and $(110)_m \parallel (101)_\epsilon$, which are consistent with the numerical relations of $3c_m \approx b_\epsilon$ and $5d_{(110)_m} \approx 6d_{(101)_\epsilon}$. Figure 7b taken also from N99O1 shows that the [130] zone axis (or [310] zone axis) for mullite

(14) Schneider, H.; Rager, H. *J. Am. Ceram. Soc.* **1984**, *67*, C-248.
(15) Schneider, H.; Rager, H. *Ceram. Int.* **1986**, *12*, 117.
(16) Schneider, H. *J. Am. Ceram. Soc.* **1987**, *70*, C-43.
(17) Cardile, C. M.; Brown, I. W. M.; Mackenzie, K. J. D. *J. Mater. Sci. Lett.* **1987**, *6*, 357.
(18) Parmentier, J.; Vilminot, S.; Dormann, J. L. *Solid State Sci.* **1999**, *5*, 257.
(19) Ocaña, M.; Caballero, A.; González-Carreño, T.; Serna, C. *J. Mater. Res. Bull.* **2000**, *35*, 775.
(20) Ronchetti, S.; Piana, M.; Delmastro, A.; Salis, M.; Mazza, D. *J. Eur. Ceram. Soc.* **2001**, *21*, 2509.
(21) Soro, N.; Aldon, L.; Fourcade, J. O.; Jumas, J. C.; Laval, J. P.; Blanchart, P. *J. Am. Ceram. Soc.* **2003**, *86*, 129.
(22) Yamaguchi, K.; Kusano, Y.; Fukuhara, M.; Doi, A. *J. Chem. Soc. Jpn.* **1991**, 1073.

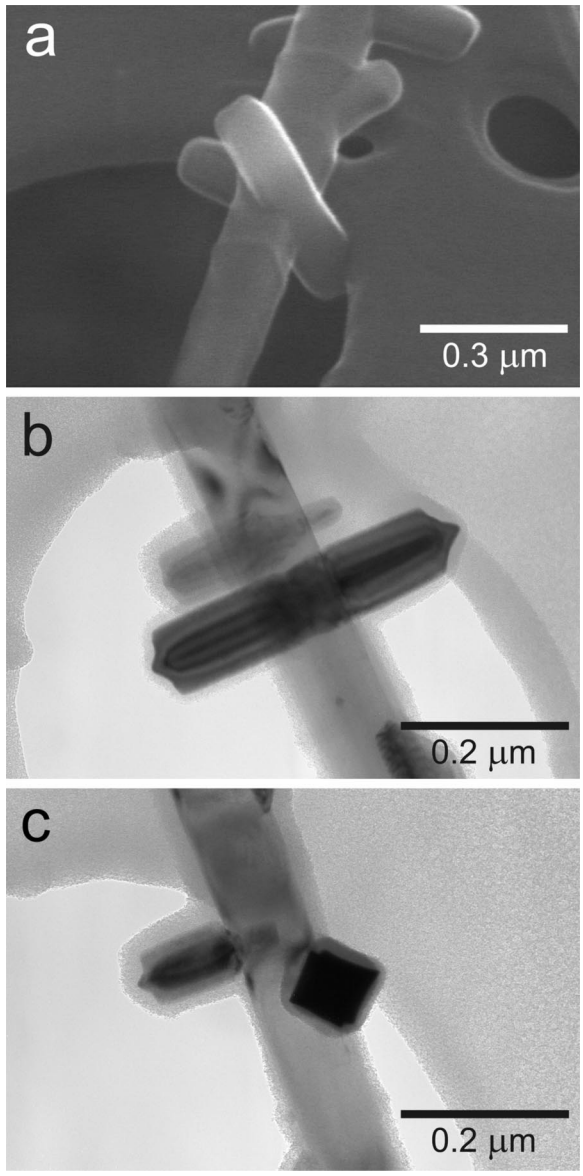

Figure 4. SEM (a) and TEM images (b and c) of the same pair of ϵ-Fe_2O_3 particles attached to a mullite crystal in N99O1 observed from different angles. The pair commonly have a square-columnar shape with prismatic ends.

corresponds to the $[\bar{1}00]$ zone axis for ϵ-Fe_2O_3, indicating an additional relation of $(\bar{3}10)_m$ [or $(1\bar{3}0)_m$] || $(001)_\epsilon$, which is consistent with the numerical relation of $4d_{(310)_m}$ [or $4d_{(130)_m}$] $\approx c_\epsilon$. We note here that it has been impossible for us to avoid the ambiguity concerning the discrimination of a_m and b_m within experimental error even with the aid of computer simulations. Anyway, the following things have become clear at least. The mullite grows along the c_m axis in a $\{110\}_m$-faceted, square-columnar shape, on which the fine ϵ-Fe_2O_3 crystals do exist along the a_ϵ axis in a principally $\{011\}_\epsilon$-faceted, square-columnar shape in the above-mentioned mutual orientation.

In Figure 7c for N98O2, on the other hand, the $[3\bar{1}0]$ zone axis (or $[\bar{1}30]$ zone axis) for mullite and the [001] zone axis for ϵ-Fe_2O_3 correspond to each other, indicating that $c_m \perp (110)_\epsilon$ and $(130)_m$ [or $(310)_m$] || $(1\bar{3}0)_\epsilon$, which are consistent with the numerical relations of $3c_m \approx 2d_{(110)_\epsilon}$ and $d_{(130)_m}$ (or $d_{(310)_m}$) $\approx d_{(130)_\epsilon}$. The ϵ-Fe_2O_3 crystals are grown in the c plane

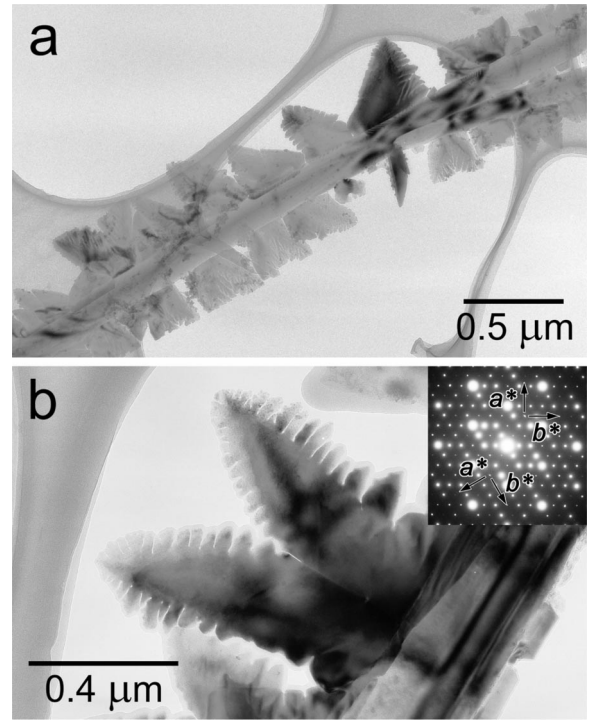

Figure 5. Typical TEM images for N98O2. The ϵ-Fe_2O_3 crystals are grown in the c plane preferentially into a dendritic, thin finlike shape. (110)-mirrored twinning such as that shown in part b was observed frequently.

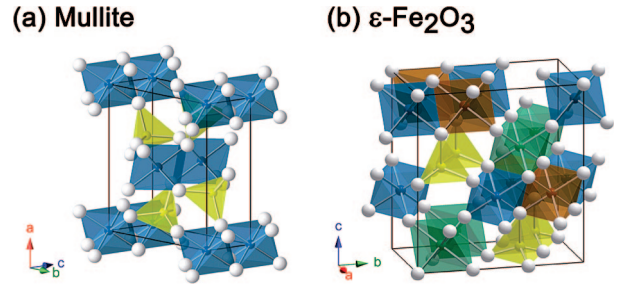

Figure 6. Schematic representation of the crystal structures of mullite (a) and ϵ-Fe_2O_3 (b). In part a, the octahedra are colored blue and the tetrahedra yellow. In part b, the octahedra are colored blue, green, and brown to indicate their crystallographic difference, and the tetrahedra are colored yellow.

preferentially. It has thus become clear that ϵ-Fe_2O_3 grows epitaxially on mullite, sensitively changing the relative orientation, shape, and size with p_{O_2}.

The two types of relative orientations are illustrated schematically in Figure 8, where parts a and b apply to N99O1 and part c to N98O2. Figure 8a shows the cross section normal to the needle axis of mullite, c_m, and also the cross section normal to the b_ϵ axis of a parasitic ϵ-Fe_2O_3 particle. The same pair of particles viewed along the a_ϵ axis is illustrated in part b. The c_m axis length of 0.2894(0) nm is equal to the Al−Al distance of a pair of edge-sharing octahedra (see Figure 6a). Looking into the structure of ϵ-Fe_2O_3 illustrated in Figure 6b, one notices that the near-neighboring FeO_6 octahedra are paired along the b_ϵ axis in the same edge-sharing manner as that in mullite. The Fe−Fe spacing is nearly 0.29 nm for all of the combinations of FeO_6 octahedra, the three times of which is equal to the b_ϵ axis length of 0.8789 nm. From this similarity in the arrangement

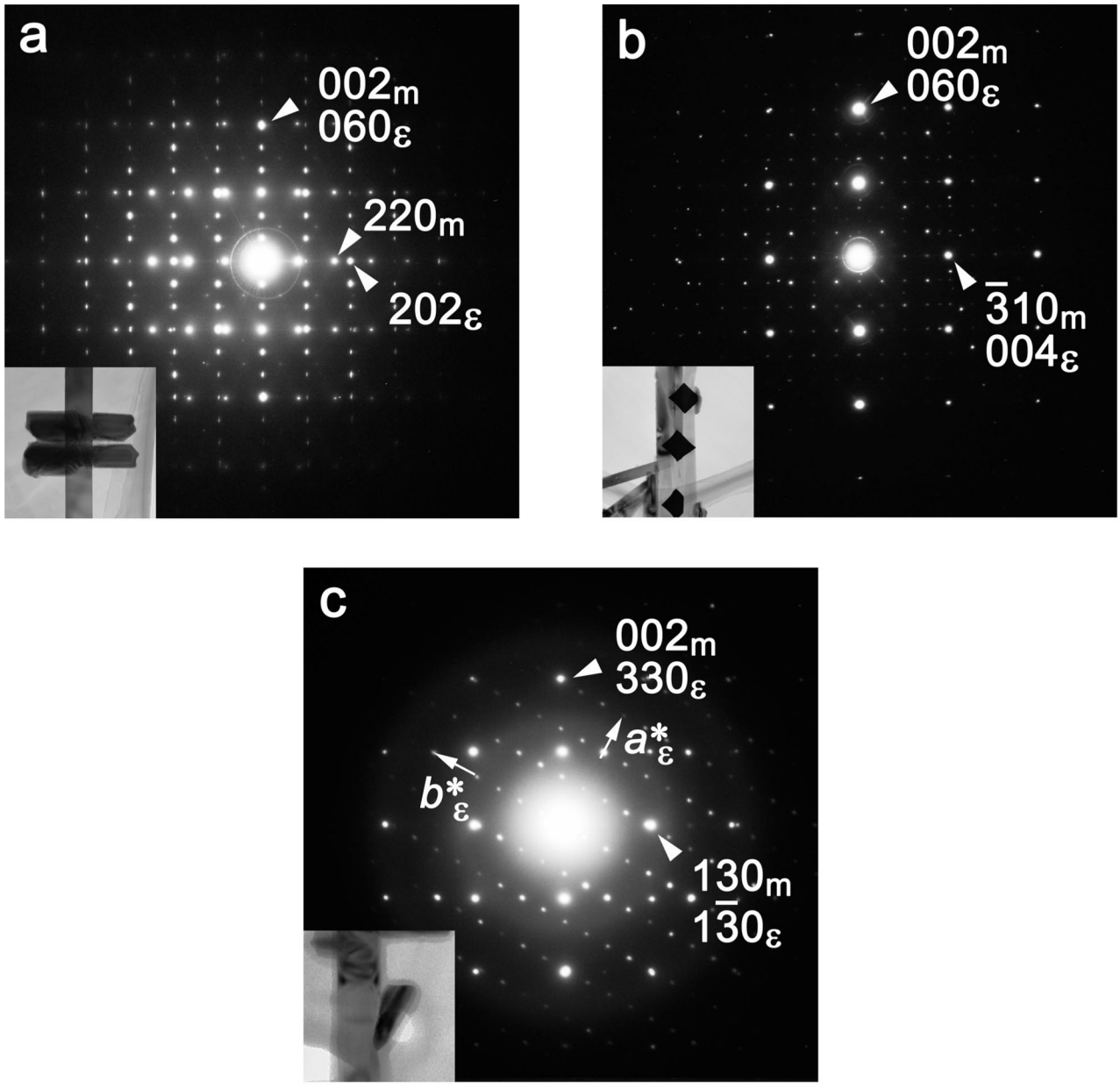

Figure 7. ED patterns taken from N99O1 showing that the [1$\bar{1}$0] (a) and [130] (or [310]) (b) zone axes for mullite correspond to the [$\bar{1}$01] (a) and [$\bar{1}$00] (b) zone axes for ϵ-Fe_2O_3, respectively. The crystallographic relationship deduced from pattern a is $c_m \parallel b_\epsilon$ and $(110)_m \parallel (101)_\epsilon$ (m = mullite and $\epsilon = \epsilon$-Fe_2O_3). Pattern b indicates $(\bar{3}10)_m$ [or $(1\bar{3}0)_m$] $\parallel (001)_\epsilon$. Pattern c from N98O2 reveals that the [3$\bar{1}$0] (or [$\bar{1}$30]) zone axes for mullite correspond to the [001] zone axis for ϵ-Fe_2O_3, from which the relations of $c_m \perp (110)_\epsilon$ and $(130)_m$ [or $(310)_m$] $\parallel (1\bar{3}0)_\epsilon$ are deduced. The corresponding particle images are shown in the insets.

of the octahedra, we can understand the directional and numerical relations of $c_m \parallel b_\epsilon$ and $3c_m \approx b_\epsilon$.

The ϵ-Fe_2O_3 particles of N98O2 have the relative orientation illustrated in Figure 8c (see the particles in Figure 7c for comparison). The lattice planes of $(001)_m$ and $(130)_m$ [or $(310)_m$)] are parallel to those of $(110)_\epsilon$ and $(1\bar{3}0)_\epsilon$, respectively. The relation of $(130)_m$ [or $(310)_m$)] $\perp (001)_\epsilon$ holds also for N99O1, but the b_ϵ axis is rotated around the c_ϵ axis by 60° to set the $(110)_\epsilon$ plane normal to the c_m axis. The frequently observed twinning results when one ϵ-Fe_2O_3 particle such as that illustrated in Figure 8c meets another, $(110)_\epsilon$-mirrored crystal.

All of the previous studies, including also the case starting from nontronite, $Na_{0.3}Fe_2(Si,Al)_4O_{10}(OH)_2 \cdot nH_2O$, studied by Wonterghem et al.,[23] reported that the presence of amorphous silica as a matrix is needed for ϵ-Fe_2O_3 to form. Parallel to these, the present molten pellet surface also contains amorphous silica, but the specialty here is that ϵ-Fe_2O_3 is provided with mullite as a substrate to grow epitaxially on. Stated more generally, the substrate changes with p_{O_2} from corundum for $p_{O_2} \geq 2$ vol % to mullite for $p_{O_2} < 2$ vol %, and the resulting iron oxide changes accordingly from α- to ϵ-Fe_2O_3. The ϵ-Fe_2O_3 particles obtained in the present work are relatively large single crystals. The fact that these crystals are more or less separated from each other made it easy to observe their morphology exactly, revealing the strong dependence on p_{O_2}. The development of sophisticated processes to attain fine morphological control is highly desired.

(23) Wonterghem, J. W.; Mørup, S.; Villadsen, J.; Koch, C. J. W. *J. Mater. Sci.* **1987**, *22*, 438.

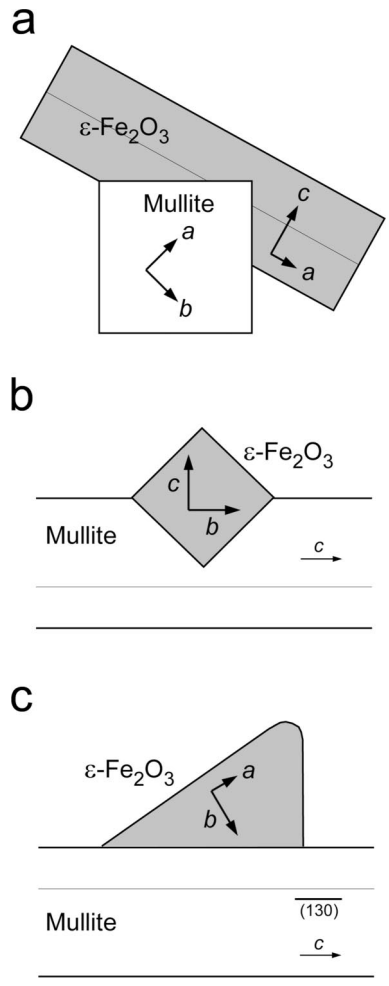

Figure 8. Schematic illustrations of the crystallographic relations between mullite and ϵ-Fe_2O_3 in N99O1 (a and b) and N98O2 (c). The *a* and *b* axes of mullite may be interchanged (see the text).

Conclusions

Relatively large ϵ-Fe_2O_3 particles grew epitaxially on needlelike mullite particles in a traditional Japanese Bizen stoneware heated with rice straw on the surface up to 1250 °C in mixed gases of $N_2/O_2 = 99/1$ and 98/2 in volume. At $N_2/O_2 = 99/1$, the particles are grown along the a_ϵ axis in a principally $\{011\}_\epsilon$-faceted, square-columnar shape with prismatic ends, and the crystallographic relations to mullite are $c_m \parallel b_\epsilon$ and $(110)_m \parallel (101)_\epsilon$. The particles at $N_2/O_2 = 98/2$ have a finlike dendritic shape grown in the *c* plane and oriented as $(001)_m \parallel (110)_\epsilon$ and $(130)_m$ [or $(310)_m$] $\parallel (1\bar{3}0)_\epsilon$. The maximum particle size of ~0.3 μm in width and ~1 μm in length is the largest one reported to date. The dependences of color and microstructure on the oxygen partial pressure during heating will be reported in further detail elsewhere in the near future.[24] ϵ-Fe_2O_3 has potential as a magnetic material. We believe that the present results will prove useful to morphological control of particles and also to devicing in the form of, for example, single-crystalline particles or films grown on mullite substrates.

Acknowledgment. The authors are indebted to Prof. H. Nishido (Okayama University of Science) for helpful discussions. This study was supported by a Grant-in-Aid for Scientific Research (C) of the Ministry of Education, Culture, Sports, Science and Technology, Japan (No. 19550199), and also by a grant from the same ministry numbered Grant 17105002.

Note Added after ASAP Publication. This paper was published ASAP December 11, 2007 with an error in the discussion of Figure 7 paragraph, and in the Figure 7 caption; the corrected version published ASAP December 13, 2007.

CM7023247

(24) Kusano, Y.; et al., in preparation.